EARTH SURFACE PROCESSES AND LANDFORMS
Earth Surf. Process. Landforms **43**, 2948–2963 (2018)

Published online 20 August 2018 in Wiley Online Library
(wileyonlinelibrary.com) DOI: 10.1002/esp.4437

Living landscapes: Muddy and vegetated floodplain effects on fluvial pattern in an incised river

Maarten G. Kleinhans,[1]* Bente de Vries,[1] Lisanne Braat[1] and Mijke van Oorschot[1,2]
[1] Faculty of Geosciences, Utrecht University, Princetonlaan 8A, 3584 CB, Utrecht
[2] Deltares, PO Box 177, 2600 MH, Delft, The Netherlands

Received 23 December 2017; Revised 9 May 2018; Accepted 5 June 2018

*Correspondence to: M. G. Kleinhans, Faculty of Geosciences, Utrecht University, PO Box 80115, 3508 TC Utrecht, The Netherlands. E-mail: M.G.Kleinhans@uu.nl

ESPL
Earth Surface Processes and Landforms

ABSTRACT: Cohesive floodplain sediment and vegetation are both thought to cause meandering river patterns. Our aims are to compare the isolated and combined effects of mud and vegetation on river planform and morphodynamics in the setting of intermediate-sized valley rivers. We use a numerical model for century-scale simulation of flow, sediment transport and morphology coupled with riparian vegetation settlement, growth and mortality as functions of species traits on which flow resistance depends. Mud fluxes were predicted by excess shear stress relations in combination with the active layer formulation. We found that valley-flooding water levels increase with vegetation density, causing a higher braiding intensity rather than meandering tendency. The shear stress during floods carves channels through the muddy floodplain surface. Higher mud concentration, on the other hand, increases floodplain aggradation, reduces the overbank flow frequency and ultimately causes formation of a single-thread channel. Vegetation causes mud to deposit closer to the river channel as a levee, showing that mud sedimentation and vegetation settling mutually enhance floodplain formation. However, mud and vegetation counteract in two ways. First, vegetation enhances floodplain accretion, which ultimately increases plant desiccation for high mud concentrations. Second, vegetation increases the tendency of periodic chute cutoffs in valleys. The chute cutoffs locally reset the landscape and create new windows of opportunity for the vegetation. Surprisingly, in systems with a high mud concentration this causes hysteretic loops of vegetation cover and delayed mud deposition. Ramifications for the interpretation of Palaeozoic fluvial facies are that even rootless vegetation, capturing cohesive mud closer to the river channel to form thicker floodplain on the point bar, can enhance the tendency to meander and, under high mud supply, form stable channels. However, meandering is more unlikely in narrower valley rivers with higher vegetation density. © 2018 John Wiley & Sons, Ltd.

KEYWORDS: meandering river; pioneer vegetation; floodplain formation; mud; Palaeozoic

Introduction

Problem definition and objective

Meandering, as opposed to braiding, has been coupled to the presence of riparian vegetation and mud (see, for review, Kleinhans, 2010) in the sedimentary record (Ferguson, 1987; Bogaart and van Balen, 2000; Davies *et al.*, 2011), in experiments (Braudrick *et al.*, 2009; van Dijk *et al.*, 2013b) and in numerical modelling (Nicholas, 2013; van Oorschot *et al.*, 2016). Although there is clear evidence in present-day rivers that the combination of mud and vegetation is associated with meandering (Ferguson, 1987; Kleinhans and van den Berg, 2011), also vegetation in isolation can lead to meandering (Braudrick *et al.*, 2009), and meandering rivers can form without vegetation in experiments with cohesive sediment (van Dijk *et al.*, 2013b), and in desert environments on Earth and on Mars (Matsubara *et al.*, 2015).

How floodplain formation precisely leads to meandering remains debated. Meandering is associated with the alternate bar regime, which, in turn, is caused by a relatively narrow and deep river channel, while the transition to braiding can occur through formation of chute cutoffs (Ferguson, 1987; Kleinhans and van den Berg, 2011). It is often thought that narrowness of meandering channels relative to braided channels is mainly caused by stability of cohesive sediment with roots at the bank top in the eroding *outer* bank of migrating meanders as simulated in one-dimensional meander simulation models (Camporeale *et al.*, 2007; Parker *et al.*, 2011) (but note that these models cannot braid). However, three-dimensional experiments (van Dijk *et al.*, 2012, 2013b) and two-dimensional models (van Dijk *et al.*, 2014; van Oorschot *et al.*, 2016) for meandering rivers close to the threshold to braiding emphasize that meandering emerges following a reduction of the tendency to form chute cutoffs by floodplain formation on the *inner* bend.

Furthermore, the isolated effects of vegetation and mud on floodplain formation and destruction are not a simple function of the amount of vegetation and mud, and neither are their combined effects a simple sum of the two. This is exem-

plified in experiments (van Dijk *et al.*, 2013a) and models (van Oorschot *et al.*, 2016) that show an increase, rather than decrease, of braiding intensity with the introduction of vegetation, which forms stable bar heads that split channels persistently. The question therefore remains: under what conditions could introduction of vegetation combined with mud lead to more braiding or would cause a more meandering tendency?

The causal relations between combined floodplain-forming processes and the tendency to meander also require further investigation in view of two different contexts of living landscapes: that of river renaturalization efforts (Geerling *et al.*, 2006; Gurnell *et al.*, 2012; Straatsma *et al.*, 2017) and that of recent debate on the relation between the evolution of initially rootless land plants in the Palaeozoic and associated appearance of meandering and anastomosing rivers (Santos *et al.*, 2016; Davies *et al.*, 2017). Our aims are therefore to compare the isolated and combined effects of mud and vegetation on river planform and morphodynamics, specifically in the setting of intermediate-sized valley rivers. To this end we will use a numerical model for century-scale simulation of flow, sediment transport, morphology and vegetation.

Review and hypothesis development

Despite tremendous recent model advances, long-term two-dimensional morphological calculations for rivers with mud are rare. The runs of Nicholas (2013) were conducted with silt that was treated as sand and had no effective cohesion, whereas Schuurman (2015) modelled effects of floodplain strength by re-gridding the river channel while adding and removing floodplain by rules. Nevertheless, in both cases meandering patterns resulted, which points at the double effect of floodplain sedimentation.

First, cohesion lowers the erodibility of the banks and the floodplain. Mud is composed of cohesive clay admixed with silt and fine sand, depending on sediment supply from the hinterland. As such, it is transported high up the banks during floods and forms a cohesive sediment on the floodplain, adding strength to eroding cut-banks and to floodplain surfaces. The bank erodibility is only parametrized in meander simulation models and usually not included in two-dimensional models, with the exception of Parker *et al.* (2011), because of the importance of geotechnical processes in bank failure at a scale much smaller than the grid resolution. The lowered erodibility of the cohesive sediment on the floodplain hinders or inhibits chute cutoffs during floods that would reduce sinuosity and transition of the river towards braiding (van Dijk *et al.*, 2013b, 2014).

The second possible effect of floodplain sedimentation is that fines can accumulate to greater heights than the coarser bed sediment, which effectively reduces water depth and shear stress of flow over the floodplain to reduce chute cutoffs (Braudrick *et al.*, 2009; Schuurman *et al.*, 2013; Nicholas, 2013). In confined rivers, this increases the channel bed shear stress (e.g. Frings *et al.*, 2009). This floodplain-filling effect is well represented in numerical modelling and is perhaps at least as important as the bank stability effect. In similar environments long-term morphological modelling showed large effects of cohesive sediment on planform shapes, patterns and dynamics of deltas (Caldwell and Edmonds, 2014) and estuaries (Braat *et al.*, 2017).

Likewise, two-dimensional morphological calculations for rivers with vegetation are also scarce (see, for review, Solari *et al.*, 2016). Commonly, vegetation is parametrized as some static form of flow resistance along one-dimensional meander models (Bogoni *et al.*, 2017) or in two-dimensional models (Nicholas, 2013). Only one case is known where vegetation was allowed to settle and grow and mortality was determined by environmental conditions (van Oorschot *et al.*, 2016). Vegetation is known to enhance sedimentation (e.g. Corenblit *et al.*, 2016b) but this is not directly incorporated into models as the processes have a much smaller spatial scale than typical grid resolutions allow to represent. The effect of dynamic vegetation compared to the more simplistic 'static' vegetation was a much more dynamic and more patchy pattern of vegetation and morphology (van Oorschot *et al.*, 2016). Regardless, dense vegetation can have a similar floodplain-filling and shear stress-reducing effect as fine sediment because of the higher hydraulic resistance it induces. This requires that vegetation settles so uniformly that no long flow paths emerge where flow concentrates. However, the tendency of vegetation to form patches rather than complete and perfect covers means that channels can form and enlarge between vegetation (Tal and Paola, 2010), as is also well known for tidal marshes (Temmerman *et al.*, 2007).

The added soil stability and bank stability due to rooting (Pollen-Bankhead and Simon, 2009) has also not been incorporated into two-dimensional modelling yet, and it remains an open question how important this would be relative to flow reduction by vegetation resistance and increased threshold for erosion by cohesive mud sedimentation. Effects of rooting are perhaps most important in the cut-banks of outer bends that affect meander migration rates in highly sinuous, scroll-bar-dominated rivers. In laterally more dynamic rivers, on the other hand, the redistribution of flow on floodplains and lateral channel dynamics through cutoffs are perhaps more important. Owing to model constraints we will here ignore binding of sediment by roots and only explore cohesive effects of mud, floodplain-filling effects of mud and flow resistance effects of vegetation.

Our first hypothesis is that mud stabilizes the floodplain and decreases the rate of channel migration and frequency of chute cutoffs if deposited with sufficient thickness and sufficiently high concentration of cohesive sediment in the bed. Vegetation itself also may directly reduce flow shear stress over the floodplain to decrease the rate of channel migration and frequency of chute cutoffs. The mud deposition rate may be enhanced in the presence of vegetation that reduces flow velocity, and in turn the floodplain-filling effect may reduce the flow strength over the floodplain and thus reduce the probability of uprooting. However, in combination with the channel confinement in the valley, an alternative hypothesis arises that vegetation raises flood water levels, which increases overbank flow and the rate of channel migration and frequency of chute cutoffs.

The modelling approach will allow us to discuss the effects of rooting and the possible sedimentological impact of early land plants on Palaeozoic river patterns (Davies *et al.*, 2011). Since these plants were initially rootless, their effect on outer bank stability must have been negligible. However, if our modelling shows above-ground vegetation to capture and stabilize mud on the inner bend, then this would provide a mechanism of how early, rootless vegetation could have modified fluvial channel patterns and affected the preserved fluvial facies and architecture.

Field Site Description

Our idealized modelling is inspired by the River Allier, a tributary of the River Loire in central France, situated between Moulins and Vichy (Geerling *et al.*, 2006; Kleinhans and van den Berg, 2011; van Dijk *et al.*, 2014). Our model has been developed earlier without mud and with vegetation (van

Oorschot *et al.*, 2016), and showed similar chute-cutoff and vegetation dynamics to the River Allier. The Allier is a rain-fed river with flashy hydrographs with mean annual flood flows of about 700 $m^3 s^{-1}$ that cover the entire meander belt, and low flows more than 10 times lower. The bed mainly consists of a sandy gravel mixture with thin mud drapes on the highest parts of the floodplain on the inner bends. The entire meander belt has incised over 1 m into a much wider braidplain, of which some relief is visible on aerial photographs. On the basis of local interviews, we suspect that the incision occurred over the course of the Holocene and perhaps before the 1960s, when gravel mining was still allowed. The effect is that the active floodplain is confined between low terrace scarps that are rarely flooded. The mud supply has not been measured but must be rather low since oxbow lakes persist at least for the half-century that aerial photographs are available, and are mostly filled with organic material from the encroaching riparian trees and macrophytes. The River Allier is the last intermediate-sized river in Western Europe allowed to meander freely as it is protected as an ecologically valuable system and an example for river rehabilitation projects elsewhere. Incidentally, this situation allowed data collection on meander morphodynamics and vegetation dynamics (Geerling *et al.*, 2006; Kleinhans and van den Berg, 2011; van Dijk *et al.*, 2014; van Oorschot *et al.*, 2016, 2017; Corenblit *et al.*, 2016b).

There are no direct measurements available in the River Allier of mud concentration in the flow, mud deposition rates on the floodplain or mud resistance against erosion. Here we present some observations, conducted at the end of August 2016, for the presence of mud on the highest parts of the floodplain, providing evidence that mud concentration is low or the threshold for mud erosion is low. We estimated relative proportions of gravel (> 2 mm), sand (between 2 and 0.065 mm) and mud (< 0.065 mm) at about 70 locations along eight transects on four bends at the surface and at 0.1 m depth. This shows that the sediment may have up to 100% mud on the highest portions of the floodplain, which are usually covered by grasses, shrubs and older riparian trees (Figure 1).

The most important reason for choosing the River Allier is that this case is a dynamic chute cutoff-dominated river at the transition from meandering to braiding (Kleinhans and van den Berg, 2011). This makes the planform river pattern sensitive to the intensity of floodplain-forming processes, where the floodplain without cohesive sediment and vegetation can allow conversion to a braided river, whereas dense vegetation and cohesive sediment can induce meandering. The size and rapidity of morphological change of the river are such that strong interactions between the eco-engineering plant species and the hydromorphodynamics are expected. This river pattern is sufficiently affected by plants because they are neither sparse as in Mediterranean braided rivers, nor weak relative to the flow strength as in large rivers. On the other hand, this river pattern is not dominated by plants because they are neither overabundant as in dense forest, nor strong relative to the flow strength as in small streams. While the meander displacement rate is perhaps determined by properties of the eroding outer banks in the bends, the fastest dynamics on the scale of entire bends occur during chute cutoffs. Here, chute cutoffs are hindered by flow resistance due to vegetation on the inner-bend bar and by high bar elevations caused by overbank sedimentation (van Dijk *et al.*, 2014). These processes are likely more important than outer-bank erosion, which is fortunate because the latter is relatively poorly represented in numerical models (Schuurman *et al.*, 2018). In sum, the Allier is a dynamic, living landscape with such conditions and dimensions that its pattern is sensitive to effects of floodplain formation, allowing us a high degree of control over the most important variables that affect channel pattern.

Furthermore, the River Allier is a modestly sized river that may serve as an analogue for Palaeozoic river systems with the first land plants in Earth's history. The Allier is fairly close to its hinterland and has channel dimensions that are not too large to recognize in outcrops. On the other hand, the river is large enough to have sufficient streampower to shape the meander belt and not be hampered and deformed much by externally imposed unerodible banks, which is likely to occur in smaller systems. Although mud in the real River Allier has limited morphological significance, this paper is mostly concerned with generic effects in a modelled system with characteristics similar to the River Allier of mud on floodplain formation in the absence and presence of vegetation. We will therefore conduct a scenario-modelling study with a large range of mud concentrations to cover the entire parameter space from braided to meandering and laterally stable rivers.

Model Description

Model setup

The model used here combines the morphodynamics approach developed in Schuurman *et al.* (2013); van Dijk *et al.* (2014) and Schuurman (2015), the sand–mud interaction processes used in Braat *et al.* (2017) (based on ; van Ledden *et al.*, 2004; van Kessel *et al.*, 2011) and the vegetation dynamics developed in van Oorschot *et al.* (2016). The modelling approach, scenarios and methods of analysis are similar to those in van Oorschot *et al.* (2016) but this is the first report on the combination of cohesive mud and vegetation as floodplain-forming processes. Mathematical descriptions of the models are given in the above references and are summarized briefly below.

We used the open source Delft3D (4.01.00) code for hydro-morphodynamic modelling with depth-averaged flow, sediment transport and bed-level update (Lesser *et al.*, 2004). Delft3D has been successfully applied and validated in many unpublished engineering applications in fluvial, estuarine, deltaic and coastal systems, as well as in published scientific applications and idealized model studies (e.g. van der Wegen *et al.*, 2010; Schuurman, 2015; van Oorschot *et al.*, 2016).

Hydrodynamics were calculated in two dimensions by solving the Navier–Stokes equations for incompressible fluid with Boussinesq and shallow-water assumptions, including the continuity equation and the momentum equation. These require an upstream boundary condition of discharge, a stage–discharge relation at the downstream boundary such that flow is approximately uniform, and a constitutive relation for flow resistance that here includes the friction caused by vegetation.

The vegetation model was built by van Oorschot *et al.* (2016) in MATLAB (R2013b) and separately predicts vegetation colonization, growth and mortality through flooding, desiccation, uprooting, scour and burial. The hydraulic resistance for each model grid cell is calculated as parallel resistors for all age classes on the basis of vegetation stem diameter, number of stems, vegetation height and occupation fraction (Baptist *et al.*, 2006). Two generic riparian tree types are included that were inspired by poplar, which is more sensitive to inundation, and willow, which is more sensitive to desiccation. Vegetation parameters were the same as in van Oorschot *et al.* (2016) (Table I). The settling occurs only in the recruitment season at locations where the bed was moist. Growth is modelled as a logarithmic function of age. Plants unaffected

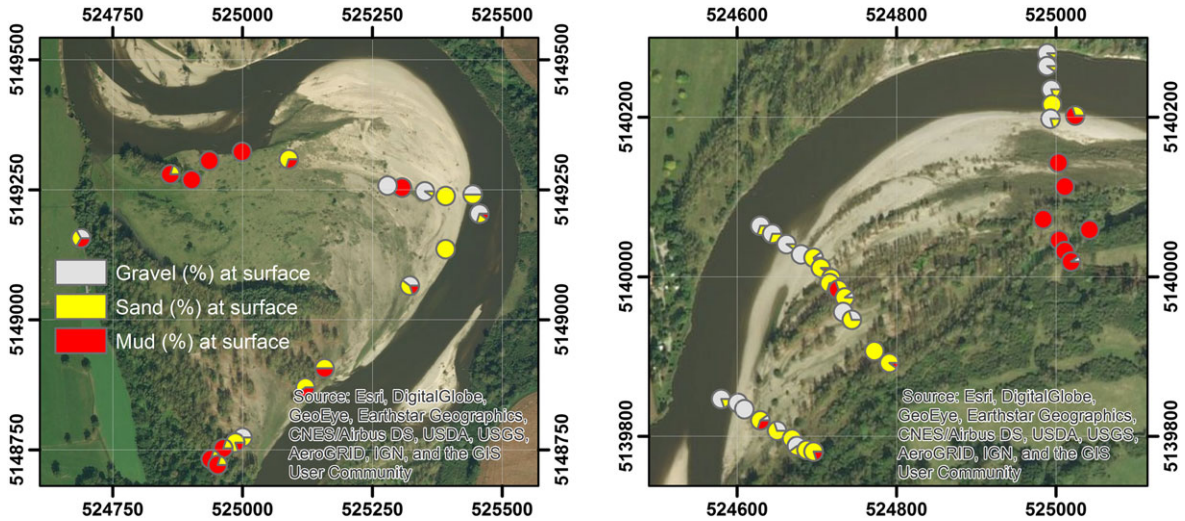

Figure 1. Two examples of meander bends in the River Allier, France, showing estimated proportions of mud (red), sand (yellow) and gravel (grey) at the bed surface collected in August 2016. Aerial photography coordinates WGS84 in UTM31T. General flow direction is from south to north.

Table I. Generic vegetation characteristics (source: van Oorschot *et al.*, 2016)

Parameter	Unit	Willow seedling	Willow forest	Poplar seedling	Poplar forest
Maximum age	y		60		150
Root length	m	0.10	0.85	0.50	1.15
Shoot length	m	0.25	11.5	0.10	14.0
Shoot stem diameter	m	0.002	0.41	0.036	0.60
Timing of seed dispersal	Month	June		May	
Number of stems	m^{-2}	25	0.16	25	0.27
Area fraction	—	0.8	0.8	0.8	0.8
Drag coefficient	—	1.0	1.5	1.0	1.5
Desiccation threshold	Days	25	240	35	260
Flooding threshold	Days	70	310	60	290
Ripping threshold	$m\,s^{-1}$	0.55	12	0.55	12

Note: Except for maximum age, the parameters are given for the seedlings that the most frequently occurring life stage and, for comparison, for 10-year-old trees at the onset of the forest life stage (see Table II in ; van Oorschot *et al.*, 2016, for complete parameter set and original sources). Seedlings are .

by morphodynamic pressures die due to senescence when their maximum age is reached. Mortality by flooding, desiccation, uprooting, scour and burial are life-stage dependent, as younger vegetation is more sensitive to morphodynamic pressures. Flooding, desiccation and uprooting mortality is calculated with the dose–effect relations described in van Oorschot *et al.* (2016). Burial occurs when the amount of sedimentation exceeds the shoot height, and scour occurs when the amount of erosion exceeds the rooting depth, both of which are age dependent. Vegetation settling, growth and mortality are evaluated yearly.

The sediment transport is modelled exactly as in Braat *et al.* (2017). This means that the capacity transport predictor of Engelund and Hansen (1967) is used for a bed composed dominantly of sand, and transverse bed-slope effects are applied to this transport component. Starting from an initial bed surface bed level and pure sand composition, bed-level change was calculated from the gradients in sediment transport. Dry cells adjacent to eroding cells were attributed 50% of the erosion to allow cut-bank erosion. However, most of the outer-bank erosion occurs in submerged conditions during floods and proceeds by the transverse bed-slope effect. The bend migration rate is therefore sensitive to the bed-slope effect (Schuurman *et al.*, 2018), but as the bed-slope effect also determines bar length we chose the value that reproduces the meander bend length of the Allier best (van Oorschot *et al.*, 2016) and is near the optimal value for bank erosion in Schuurman *et al.* (2018). Consequently, the bend migration rate in the model includes a crude approximation of the cut-bank retreat processes that take place at subgrid scales.

Sediment is considered to be cohesive above a critical mud mass fraction in the bed surface. While mud in nature is a mixture of clay, silt and fine sand, here it is represented by a single settling velocity and erosion threshold and a minimum mud concentration of 40% in the bed for cohesion-dominated behaviour. Cohesive sediment is considered to be suspended and is described by the advection–diffusion equation. The Partheniades–Krone excess shear stress relations predict erosion and sedimentation; see Table II for sediment parameters and Table III for morphological and numerical parameters (van Ledden *et al.*, 2004; van Kessel *et al.*, 2011; Le Hir *et al.*, 2011). The balance of erosion and sedimentation determines the bed elevation change. Mixtures of sand and mud in the modelled bed are treated as follows. When the bed is cohesive, determined by a critical mud mass fraction in the bed, the mud and sand fluxes are proportional to the mud and sand fraction in the bed, but the erosion rate for sand is based on the entrainment of mud, because the sand particles are included in the cohesive matrix that is dominated by mud characteristics (Mitchener and Torfs, 1996; Winterwerp and van Kesteren, 2004). In this way sand can only be eroded when mud is eroded.

To track the mud and sand fractions in the bed, an active layer and bed-layer storage module were used (van Kessel

Table II. Default sediment characteristics applied in the models with sand and mud. The mud erosion threshold and the upstream sediment concentration were varied in the scenarios around the default values given here

Sediment property	Symbol	Value	Unit
Sand			
Median grain size	D_{50}	5×10^{-3}	m
Specific density	ρ_s	2650	$\mathrm{kg\,m^{-3}}$
Dry bed density	ρ_{dry}	1600	$\mathrm{kg\,m^{-3}}$
Mud			
Upstream concentration	c	20	$\mathrm{g\,m^{-3}}$
Settling velocity	w_S	2.5×10^{-4}	$\mathrm{m\,s^{-1}}$
Critical bed shear stress for sedimentation	$\tau_{\mathrm{crit,sed}}$	1000	$\mathrm{N\,m^{-2}}$
Critical bed shear stress for erosion	$\tau_{\mathrm{crit,ero}}$	0.2	$\mathrm{N\,m^{-2}}$
Erosion parameter	M	1×10^{-4}	$\mathrm{kg\,m^{-2}\,s^{-1}}$
Specific density	ρ_s	2650	$\mathrm{kg\,m^{-3}}$
Dry bed density	ρ_{dry}	1600	$\mathrm{kg\,m^{-3}}$

Table III. Parameters for model processes and numerics

Parameter	Unit	Value
Time step	min	0.3
Spin-up time at cold start	min	1.44×10^4
Threshold depth for drying/flooding	m	0.08
Min. water depth for bed-level change	m	0.1
Erosion fraction of adjacent dry cells	—	0.5
Morphological acceleration factor	—	30
Transverse bed slope constant	—	0.7
Transverse bed slope power	—	0.5
Bed storage layer thickness	m	0.1
Active layer thickness	m	0.03

et al., 2011; Braat *et al.*, 2017). Sediment exchange with the water column occurs through the active layer, which had a constant thickness and moved through the vertical framework with bed aggradation and degradation. Below the active layer, a number of stacked layers stored bed composition (Table III). The use of the active layer means that even a pure mud layer deposited on a sand-bed would mix in, such that the mud concentration depends on the active layer thickness and the aggradation by the mud layer. It would therefore take a deposit with a thickness of a few times the active layer thickness to attain 100% mud concentration in the bed surface layer.

Model scenarios

Idealized initial and boundary conditions are inspired by those in the River Allier as follows. The model domain is about 3600 m long and 1000 m wide with 25 m square grid of cells. The initial bed surface has the same initially specified set of symmetrical bends as in van Oorschot *et al.* (2016) because we focus on the development of river pattern rather than the initiation of meandering. We specified three sine-shaped meander bends with similar dimensions to the River Allier and a sinuosity of 1.39 and a valley gradient of 3.3 $\mathrm{m\,km^{-1}}$. The wavelength of the bends was calculated from a linear stability theory for forced bars (Struiksma *et al.*, 1985) that uses the same formulations as the Delft3D model (van Oorschot *et al.*, 2016). This is exactly the same initial condition as in van Oorschot *et al.* (2016). Some minor parts of the bed surface were accidentally nearly horizontal, such that a thin layer of water remained there after cold-starting the model with a high water level, which prevented dry cell erosion. This may have hampered meander migration slightly in the original modelling (van Oorschot *et al.*, 2016) that we here removed by cold-starting the model with a lower water level.

Table IV. Model scenarios

Run	Vegetation	Mud supply ($\mathrm{g\,m^{-3}}$)	Critical mud fraction —	Critical shear ($\mathrm{N\,m^{-2}}$)	Active layer (m)
1	Yes	20	0.4	0.2	0.03
2	Yes	0	na	na	na
3	No	20	0.4	0.2	0.03
4	No	0	na	na	na
5	Yes	5	0.4	0.2	0.03
6	Yes	50	0.4	0.2	0.03
7	Yes	100	0.4	0.2	0.03
8	Yes	500	0.4	0.2	0.03
9	Yes	20	0.4	0.1	0.03
10	Yes	20	0.4	0.5	0.03
11	Yes	100	0.4	0.5	0.03
12	Yes	500	0.4	0.5	0.03
13	Yes	800	0.4	0.5	0.03
14	No	500	0.4	0.5	0.03
15	Yes	20	0.2	0.2	0.03
16	Yes	20	0.6	0.2	0.03
17	Yes	20	0.4	0.2	0.10

We specified a 300-year time series of discharge between 50 and 400 $\mathrm{m^3\,s^{-1}}$ composed from five typical flood hydrographs sampled in random order that vary in timing and duration that the species are sensitive to (van Oorschot *et al.*, 2016). In the initial conditions the channel is 200 m wide in high flow and 75 m wide in low flow, with depths of 3 and 1.2 m and flow velocities of 1 and 0.6 $\mathrm{m\,s^{-1}}$. The initial bed composition in the entire domain is 100% sand and we tested scenarios with a range of mud concentrations supplied at the upstream boundary. Flow was calculated with 12 s time steps, and the bed level was calculated every 6 min by multiplication of the morphological change by a morphological acceleration factor of 30, which is consistent with our earlier vegetation modelling so that results can be compared. This allowed us to do 300 year tests at reasonable computational cost, while earlier work showed this factor not to appreciably change the results (Roelvink, 2006; Schuurman *et al.*, 2013).

Bed-level statistics, maximum water levels, sinuosity and meander migration rate were calculated as described in van Oorschot *et al.* (2016). To exclude effects of boundary conditions, 500 m (20 grid cells) were trimmed off the upstream and the downstream boundaries of the morphodynamics and vegetation maps before statistics were calculated. Sinuosity and channel migration were calculated from the main channel location, which was determined from the filtered path of maximum flow velocity. Channel migration was calculated from a cross-correlation of down-valley displacement of the main channel centreline in 10-year steps. The braiding index was determined as the mean number of channels over the cross-section in which the flow velocity exceeded 0.3 $\mathrm{m\,s^{-1}}$ in December – which means winter with high discharge – and June – which represents summer conditions with low discharge. The median of the bed elevation, detrended by valley slope, was calculated to represent the entire meander belt level, and the fifth percentile of bed elevation was used as indicator for channel thalweg depth. Grid cells are considered cohesive when the mud fraction in the top layer exceeds 40%.

We ran two sets of scenarios and some additional sensitivity runs (Table IV). The first was a set of combinations with default mud parameters: a run with a pure sand-bed without mud and without vegetation as a control run, a run with mud, a run with vegetation, and a run with the combination of mud and vegetation. The second was a set with variations in the upstream mud concentration and in the erosion threshold for mud, because the default mud was rather weak, so that its morphological effects could be considered conservative. Additional runs were conducted to test sensitivity to the active layer thickness and critical mud content for cohesive behaviour.

Results

Isolated and combined effects of mud and vegetation

The effects of the low default mud concentration in isolation are minor. The morphology is fairly similar to that without mud and without vegetation (Figure 2), but with a lower braiding index both in summer and winter flow conditions (Figure 3; see also online supplementary movies, provided as supporting information). After about 70 years the bed level of the channels, here represented by the 5% percentile of detrended bed elevation, is raised as sinuosity drops and the braiding index increases in both the control run and the run with mud only, because at this point all initial meanders have been cut off (Figure 3). A thin drape of mud is only preserved near the valley walls in the 'embayments' left by cut-off meanders but insignificant in the more active zone. This mud layer expanded in extent during the first 200 years to a cover of about 10% of cohesive surface, while the spatial average mud fraction in the top layer did not much exceed 10% after 100 years (not shown). This means that the sediment remained non-cohesive in most of the reach.

The effects of vegetation compared to the bare sand-bed river are much larger, in that the river is more confined to a single large channel with higher sinuosity (Figure 2) and more variable sinuosity due to repeated chute cutoffs (Figure 3). The braiding index during winter in the vegetated runs is almost twice as large as in the models without vegetation (Figure 3) because we determined the braiding index during flood conditions with a rather low threshold velocity for channel identification, meaning that all former and incipient channels in addition to the main active channel are counted in the braiding index. The braiding indices during summer are similar and low, but sinuosity shows much higher peaks in the vegetated runs. The vegetation cover is highly variable in time, which is due to the sensitivity of settling and seedling mortality to the timing and duration of the floods. In the online movies this can be seen as temporary increases of vegetation cover in the small channels and lower parts of the fluvial plain. The majority of the seedlings disappear due to desiccation, while flooding and uprooting remove minor fractions, and scour and burial occur even more infrequently. Willow and poplar show fairly similar trends and are not shown separately.

The combined effects of mud and vegetation are not strikingly different in map view (Figure 2 and online movies), but surprising in that the vegetation cover and mud fraction are somewhat complementary: the more mud, the less vegetation in general (Figure 4; but see discussion below on cyclicity). Furthermore, the sinuosity peaks are less frequent but higher than in the vegetation run without mud between year 100 and 300 (Figure 3). The migration rate decreases towards the end, in a pattern similar to that of the run with only mud but unlike the run without mud, while the braiding index during flood conditions increases towards the end, unlike any other run. The cohesive surface cover (not shown) is about the same as that of the run with mud alone but takes a longer time to attain this level and is more variable in time. The movie (online supplement) indicates that the run with vegetation and mud became a river with an anastomosing pattern with a rather stable channel network that was activate during floods, had deeper channels than the runs without vegetation and occasionally formed a strongly meandering main channel with sinuosity peaks up to 2.5 (Figure 3).

Both the vegetation and mud cover increase over time, but not in straightforward proportionality. The hysteresis loops show that vegetation cover increases first, after which mud is captured (Figure 5A). This does not conflict with the earlier observation that higher mud concentrations lead to lower vegetation covers in general for the entire domain, because for nearly all mud concentrations the floodplain develops hysteretically over time, while vegetation cover increases, only much less so with higher concentration.

The hysteresis loops emerge as follows. The vegetation cover fluctuates due to floods and subsequent desiccation on higher parts of the fluvial plain. Furthermore, vegetation cover appears quasi-cyclic because of the repeated chute-cutoffs in the river, which is illustrated in the relation between vegetation cover and sinuosity (Figure 5B). Cutoffs cause vegetation mortality where the river seeks a new course, which causes a drop in water level during subsequent floods and leads to the abandonment of a low area. The drop in water level leads to higher vegetation mortality due to desiccation. The lowered overbank area along the new course provides a window of opportunity for the vegetation to settle and survive desiccation stress, while the abandoned low areas provide a sheltered environment where vegetation ages considerably. The delayed peaks in mud cover correlate best with the peaks in vegetation cover of the new bushy vegetation that develop in the 2–10 years following floods and chute cutoffs. The model shows that bushy vegetation is especially effective in capturing mud on the floodplain, which is caused, first, by the fact that bushy vegetation causes the highest flow resistance, secondly by its large cover on the floodplain, and thirdly because bushy vegetation persists long enough to form a significant mud deposit that would otherwise have washed away with the seedlings in the high flood flows. This does not mean that mud is not deposited elsewhere. The hysteresis loops are counter-clockwise (Figure 5A), which shows that mud cover is still increasing when the vegetation cover is already decreasing due to ageing and mortality. Regardless of cause and effect, this means that the mud deposits remain dynamic.

The presence of vegetation leads to a different spatial pattern of mud deposition compared to the mud-only run (Figure 6; compare runs 1 and 3). Mud in isolation deposits mostly at the flanks of the valley where the morphodynamics are lower and the uneroded terrace highs provides shelter against the flow. However, in the presence of vegetation, the mud spreads quite evenly over the floodplain as a function of distance from the channel. This is probably caused by the decrease in flow velocity outside the channels by the riparian vegetation, which itself grows more frequently closer to the river channel given its sensitivity to desiccation in these settings.

Effects of upstream mud concentration and erosion threshold

The effects of higher mud concentration supplied at the upstream boundary are quite large. The higher the mud con-

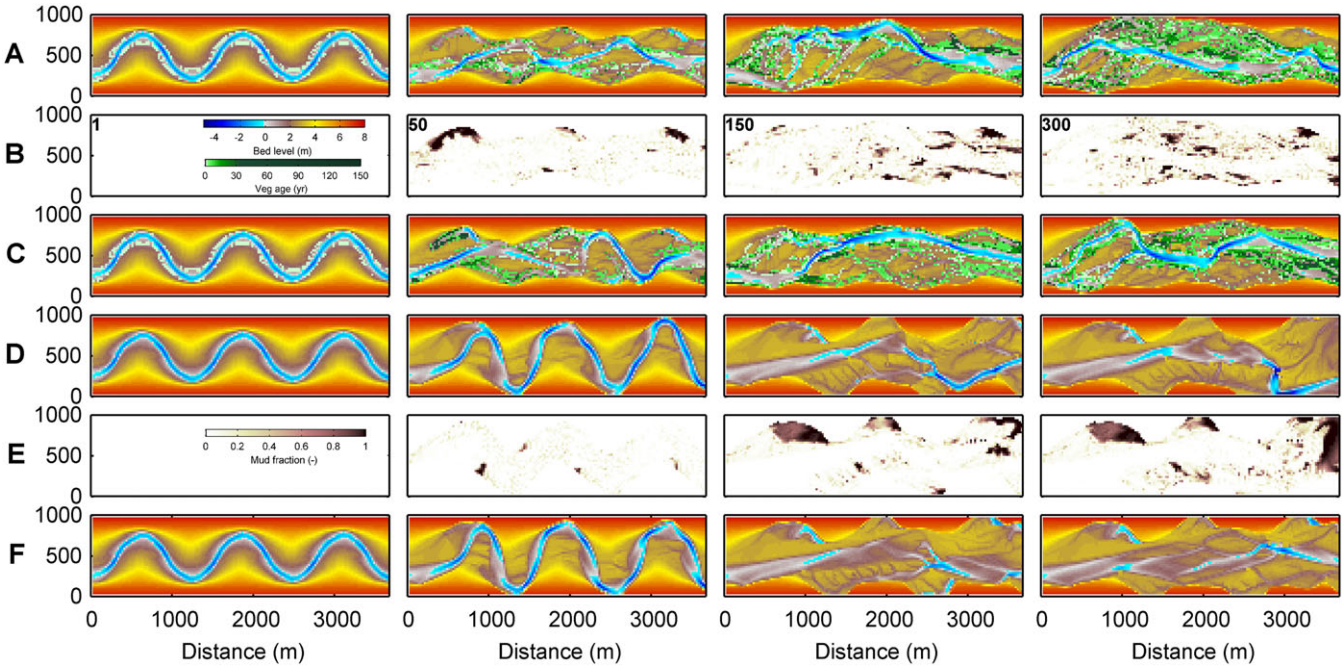

Figure 2. Maps of detrended bed elevation overlain by vegetation age and of mud fraction in the bed surface for model run 1 with vegetation and mud (A, B), run 2 with vegetation (C), run 3 with mud (D, E) and run 4 with sand only (F) (see Table IV).

centration, the more the river concentrates into a single channel (Figure 7), while lateral channel mobility and sinuosity decrease (Figure 8). In particular, the extremely high mud concentration of 500 g m^{-3}, which is also more cohesive, leads to a higher median bed level than the other runs, while the channels have the same bed level, meaning that the higher mud supply caused higher floodplain sedimentation. This reduced the vegetation cover (Figure 4A) because the flooding frequency decreases, the settling reduces and mortality due to desiccation increases. Note that effects of soil composition on desiccation of plants are not incorporated into the model, and neither are other species that would settle under such reduced flooding and desiccation stress conditions.

The effects of a higher or lower critical threshold for mud erosion are fairly limited in the default, low-mud concentration runs. Concentrations in the top bed layer are higher with a higher erosion threshold. The vegetation cover is similar for these runs (Figure 4B), showing that vegetation strongly affects mud trapping in the floodplain, but mud does not enhance vegetation settlement because this effect is not included in the model.

The combination of a higher mud concentration and a higher erosion threshold have a disproportionally larger effect on the bio-geomorphodynamics than either of the two variables in isolation. For the high erosion threshold, the vegetation cover reduces dramatically with increasing mud concentration and only flanks the main channel in a narrow zone for a concentration of 500 mg L^{-1} (Figure 7). The braiding index even during floods is low, as are lateral channel mobility and sinuosity (Figure 8). The highest mud concentrations lead to very high and barely flooded floodplains that harness the river into a single, deep and narrow and rather static straight channel. This channel is flanked by very little riparian pioneer vegetation. On the other hand, in the same concentrations but with a lower erosion threshold the channel remains dynamic and the vegetation cover is much larger and dynamic.

After 100 years the high mud concentration and high erosion threshold lead to meanders with a lower amplitude and dynamics focused in the centre of the valley (compare Figures 8 and 3). This caused the large initial meanders formed in the first stage to function as oxbow lakes that efficiently trapped mud and eventually were preserved under a thick deposit (Figure 9). The sinuosity and migration reduced when the initial bends were cut off, while sinuosity peaks were much less high and less frequent, showing that the high mud concentration removes the tendency to meander.

The effects of mud concentration and erosion threshold for all runs on the bio-geomorphodynamics are summarized in Figure 10. The expected effect of increasing mud concentration and increasing mud strength is a decrease of braiding index and a transformation from a braided river without mud and vegetation to a dynamic meandering river with mud and vegetation. At the same time, the lateral channel mobility changes in style from meander migration to more sudden channel displacement. For the highest concentrations a straight, immobile river with very little vegetation emerges. However, a counterintuitive effect is that higher vegetation covers have a higher braiding index during floods, except for high mud concentrations. Furthermore, the summary does not show the important order of floodplain formation: first, timing and magnitude of floods and occurrence of chute cutoffs create windows of opportunity for vegetation settling that are determined by flood timing and magnitude and by occurrence of chute cutoffs (Figure 5B). After that, mud cover increases (Figure 5A) and may, depending on concentration, fill up the floodplain to such an extent that overbank flow frequency and extent reduce so that pioneer vegetation no longer settles away from the channel margin.

Discussion

Interpretation

The model results are evidence for combined effects of mud sedimentation and vegetation settlement on meandering that are stronger than, and different from, the effects of either mud or vegetation in isolation. A low mud concentration causes a larger vegetation cover after the first century of model time, and while the mud cover on the surface is similar, the mud

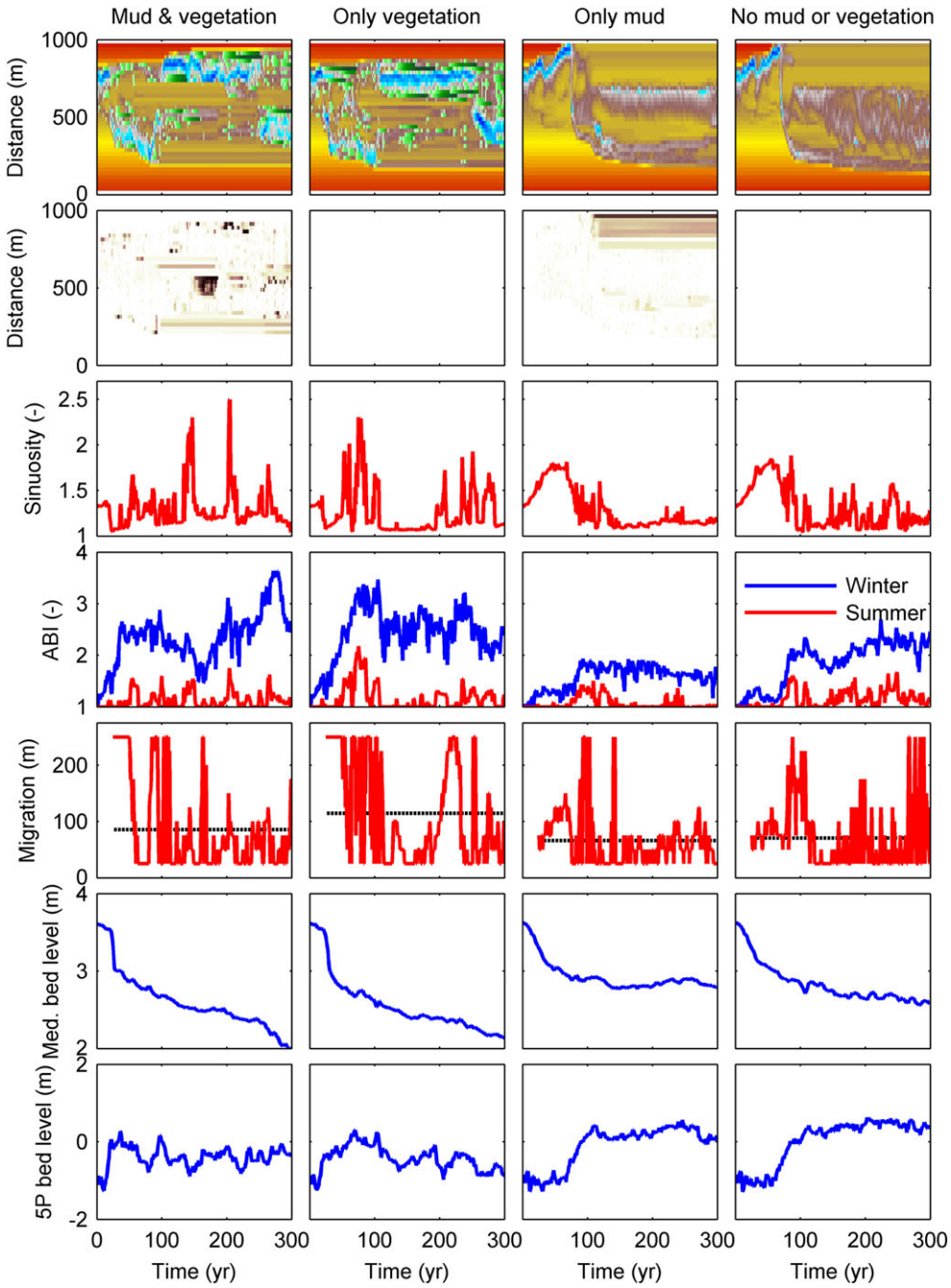

Figure 3. Development of the morphology in model runs 1–4. Top two panel rows: bed level, vegetation age and mud cover in the center cross-sections (see Figure 2 for legends). Lower panel rows with characteristics of morphology: sinuosity of the main channel identified from the flow velocity field, braiding index for summer and winter water levels, channel migration rate of the summer channel, and median and 5% percentile of the detrended bed level characterizing meander belt bed level and thalweg bed level.

deposited closer to the river channel in the presence of vegetation to enhance levee formation. In other words, the effect of the combined presence of mud and vegetation is a stronger floodplain in the inner bends. This enhances the tendency to meander because it reduces the chute cutoff tendency, but only up to a certain point, after which relatively higher mud concentrations reduce the meandering tendency because sinuosity is reduced. This trend is in general agreement with the literature (Ferguson, 1987; Makaske, 2001; Kleinhans, 2010; Kleinhans *et al.*, 2012; Nicholas, 2013).

Isolated and combined effects of mud and vegetation

The floodplain is affected by the confinement in the incised valley, in particular in combination with the vegetation. Here, confinement is suggested to occur if discharges lower than the mean annual peak flood the valley width or the width of a corridor confined by natural or artificial levees. Spatial non-uniformity of the vegetation cover leads to further focus of flow into poorly defined floodplain channels or water pathways, which was captured in the braiding index determined by flow velocity during floods. The effect is a reduction of sedimentation: where the run with only mud shows a higher median bed level than the control run without mud and without vegetation, the runs with only vegetation and with combined vegetation and mud continue to lower the median bed level as the higher terraces are removed by lateral channel activity. This is interpreted to be the effect of flow focus by vegetation and higher flood water levels, both of which enhance erosion. On the other hand, mud without vegetation reduces floodplain lowering because of its higher threshold for erosion

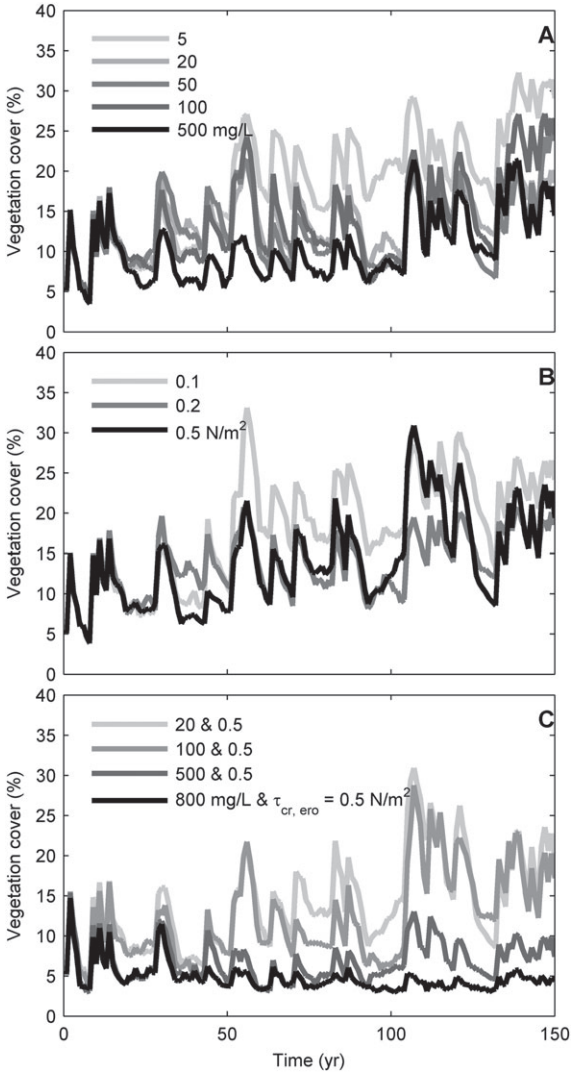

Figure 4. Development of area covered by cells containing vegetation for mud scenarios: (A) effects of mud supply; (B) effects of the threshold for mud erosion; (C) effects of mud supply with a higher threshold for mud erosion.

and lower flow shear stress due to lower flood water levels. Furthermore, a higher mud concentration effectively means a higher sediment supply.

The lateral channel dynamics in incised rivers with vegetation are likely higher than in unconfined rivers with vegetation because of higher flood water levels. These are caused by vegetation in combination with the flood flow confinement in the incised valley, which requires that the valley is narrow enough to cause significant flow depth increase in typical floods. This agrees with field observations where floodbasin hydraulics affected the lateral extent of levees (Filgueira-Rivera *et al.*, 2007). There are indications that these effects also occur in rivers confined by artificial levees (Frings *et al.*, 2009; Makaske *et al.*, 2011). Furthermore, there appears to be an optimal combination of lateral channel activity with vegetation density: the bushy life stage of the vegetation causes a higher flow resistance than the seedlings and mature trees, so that water levels on the floodplain are highest when the older vegetation is removed frequently enough by lateral channel dynamics, in agreement with McKenney *et al.* (1995). In a sense, the confinement of a river in a narrow valley or between artificial levees increases the disturbance energy while reducing the chances of vegetation survival, which shifts the river to a laterally more active planform pattern (Gurnell, 2014).

Emergent floodplain complexity

The settling pattern and development of vegetation lead to a more complex floodplain with strongly heterogeneous flow conditions. Only in the highest mud concentration runs does the floodplain heterogeneity smooth out. Complex floodplains lead to local flow divergence and convergence patterns, and the latter may lead to new channel incision if flow strength is larger than material strength. Floodplain complexity occurs in large rivers (Lewin and Ashworth, 2014), but is also found here because of the confinement of floodwaters in interaction with vegetation pattern formation with sufficient streampower for morphological change. Experiments with uniform seeding developed floodplain complexity with multiple flow paths and avulsion (Gran and Paola, 2001; Tal and Paola, 2010), but slight vegetation cover heterogeneity cannot be excluded. Earlier, idealized meander modelling suggested that spatial variation of vegetation could affect the meander wavelength and dynamics (Guneralp and Rhoads, 2011; Bogoni *et al.*, 2017), but more natural hydrochorous distribution of vegetation in experiments suggested much greater complexity in the spatial and temporal patterns (McKenney *et al.*, 1995; van Dijk *et al.*, 2013a), which are also observed in our modelling and field observations (Kleinhans *et al.*, this issue) and on salt marsh at an even smaller scale (Temmerman *et al.*, 2007; Belliard *et al.*, 2016). This suggests that floodplain complex-

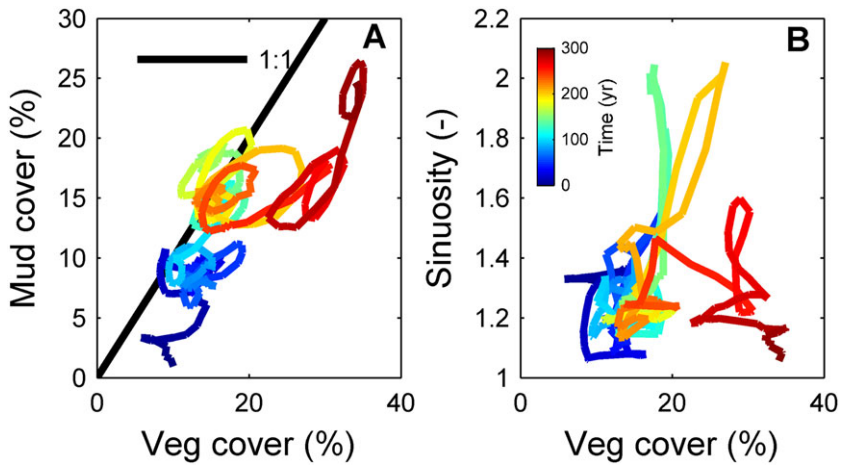

Figure 5. Mud cover (A) and sinuosity (B) plotted against vegetation cover for model run 1, with colour indicating age.

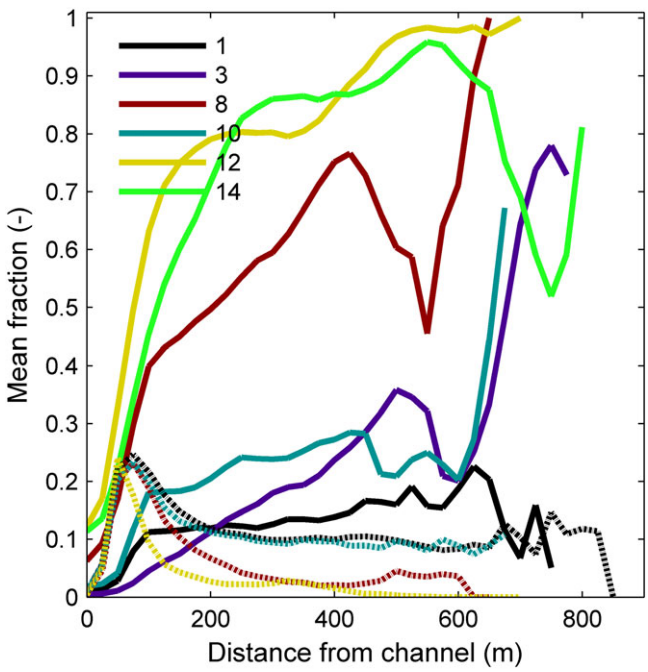

Figure 6. Vegetation (dashed) and mud (drawn) fractions in the surface layer plotted as a function of distance from the main channel, averaged over time and space.

ity *sensu* Lewin and Ashworth (2014) is not limited to large rivers but also occurs in small rivers, as long as vegetation settles non-uniformly and the flow shear stress is high enough to erode and transport sediments.

Occasionally a new channel is formed by local avulsion into a floodplain low in the model runs with high mud supply and high critical shear stress for mud erosion. This behaviour is somewhat similar to that of the anastomosing river (Kleinhans *et al.*, 2012), although the model domain is too small to form a large fluvial plain with multiple ridges. In anastomosing rivers the riparian vegetation is limited to the levees immediately adjacent to the river channels, while floodbasins capture mud for long periods of time, and avulsion rather than lateral channel migration is the main mode of activity (Makaske *et al.*, 2009), which is in general agreement with our model results that show step-like changes in migration and sinuosity rather than peaks (compare Figures 8 and 3). In other words, as the raised floodplain increasingly disconnects from the river channel, spatiotemporal variability of mud sedimentation and vegetation settlement and age distribution reduces.

Floodplain aggradation

A higher mud supply causes faster and more floodplain aggradation, on which the dynamic riparian vegetation modelled here gradually ceases to settle or dies immediately due to desiccation. Initially there was a positive feedback as vegetation reduced flow velocities, causing mud, enhancing mud deposition on the floodplain, but as the floodplain aggraded the propagules no longer arrived there. This happened despite the unlimited availability of propagules in all runs, so that vegetation cover was only limited by settling conditions and mortality. Moreover, the muddy floodplain is less susceptible to re-channelization, while lateral channel migration is also reduced. This behaviour is observed in the Garonne (Corenblit *et al.*, 2016a) and in the Rhine (Hesselink *et al.*, 2003) – both embanked rivers where lateral channel mobility is prevented by bank protection. This differs from the condi-

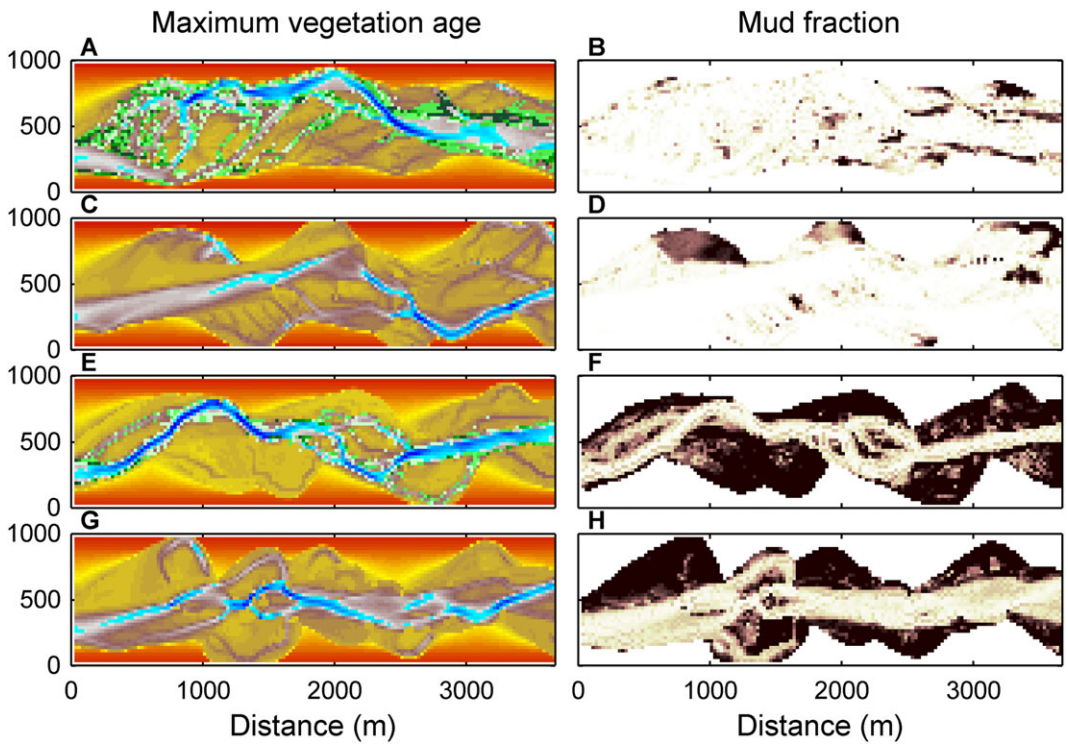

Figure 7. (A, C, E, G) Maps of detrended bed elevation overlain by vegetation age, if present, for model runs 1 and 3 with low mud concentration and runs 12 and 14 for high mud concentration after 150 years (see Table IV). (B, D, F, H) Maps of mud fraction in the bed surface layer for corresponding runs. See Figure 2 for legends.

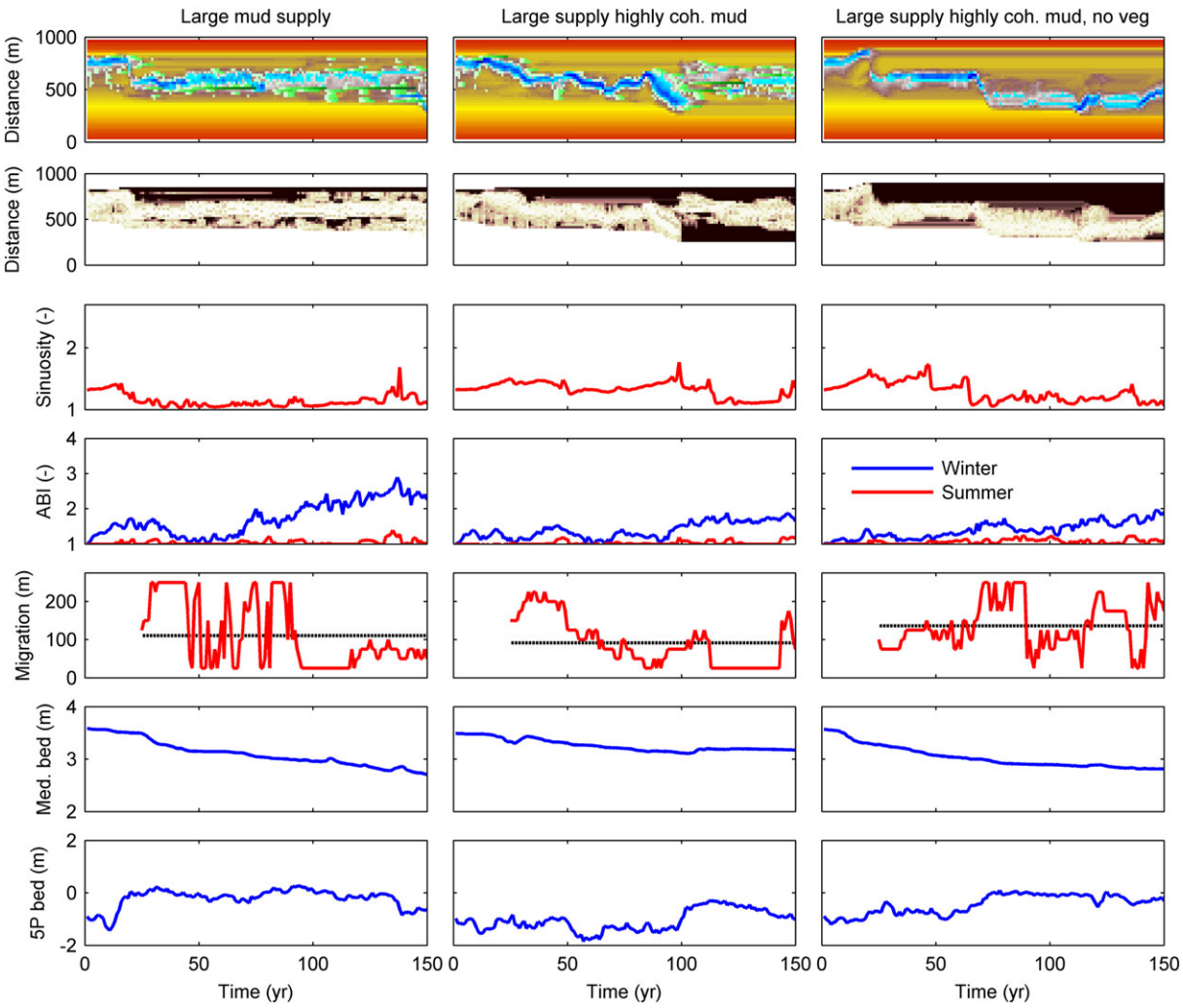

Figure 8. Development of the morphology in model runs 8, 12 and 14 with high mud concentration. See Figure 3 for explanation.

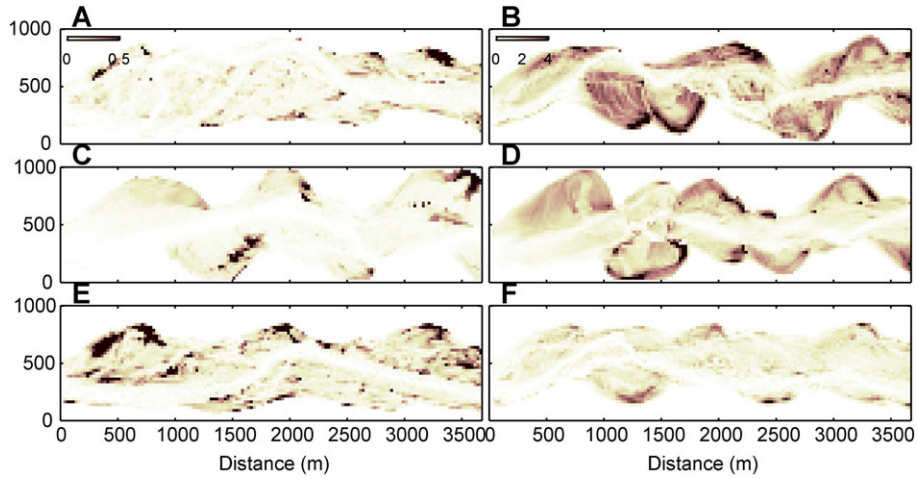

Figure 9. Cumulative thickness of mud stored in the bed after 150 years. (A) Low mud concentration with low critical shear stress for erosion, and vegetation (run 1). (B) High mud concentration with low critical shear stress for erosion, and vegetation (run 12). (C) Low mud concentration with low critical shear stress for erosion, without vegetation (run 3). (D) High mud concentration with low critical shear stress for erosion, without vegetation (run 14). Note different legends for low (left) and high (right) mud concentration runs. (E) High critical shear stress for erosion with low mud concentration (run 10). (F) Low critical shear stress for erosion with high mud supply (run 8). [Colour figure can be viewed at wileyonlinelibrary.com]

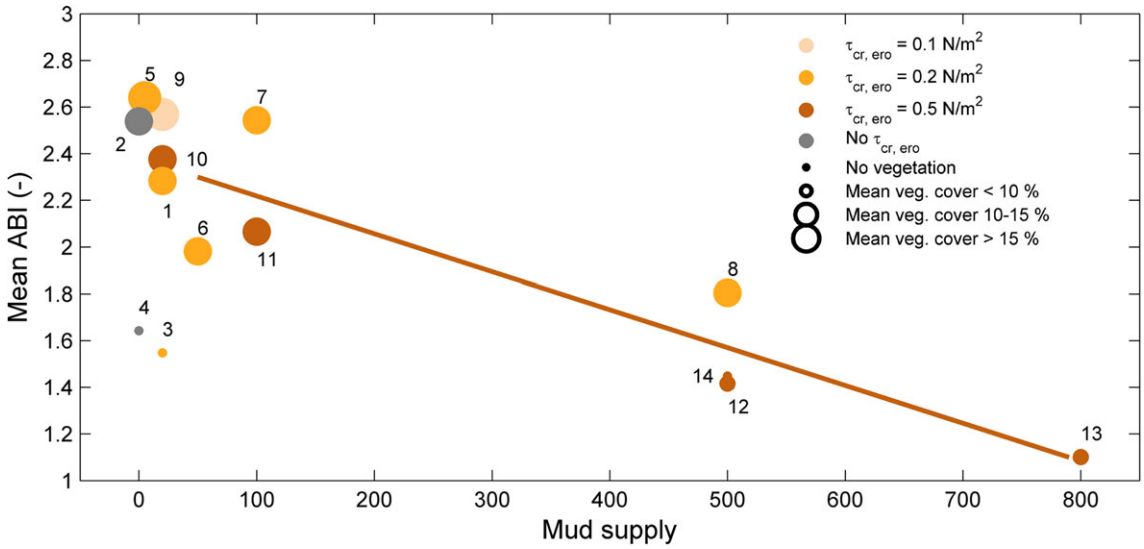

Figure 10. Effects of upstream mud concentration (mg L^{-1})) on the morphodynamics based on all model runs characterized by time-averaged braiding index determined during winter, showing a decrease in braiding index with higher mud supply and an increase in braiding index with higher vegetation cover. Symbol size indicates mean vegetation cover, and symbol colour indicates the erosion threshold for mud.

tions in more sinuous meandering rivers where the channel banks are more erodible, so that floodplain can be eroded by channel migration (Lauer and Parker, 2008). The example of the Garonne shows a strong positive correlation between total floodplain sedimentation and *Populus* age, and Corenblit *et al.* (2016a) show a spatiotemporal pattern suggesting that vegetation causes enhanced sedimentation, while surviving desiccation stress is enhanced by mud fraction in the floodplain surface.

However, presence of vegetation is not a sufficient condition for increased floodplain aggradation. Our model results suggest that lateral channel mobility also needs to be reduced, either by the vegetation and cohesive sediment, or, as in the Garonne and Rhine, by channel bank protection. Once the channel is stable, it is only a matter of time before the floodplain has aggraded up to the level of higher floods. This floodplain-filling effect then prevents cutting of new channels across the floodplain, not only because of material strength but mainly because of the lack of flow strength on the increasingly elevated and shallow floodplain as opposed to stronger flow in the confined channels. The effect is a reduction of the vegetation dynamics in agreement with our model results, although historic channel migration in the Rhine and many other rivers was hindered by groynes and riprap rather than bank cohesion (Hesselink *et al.*, 2003; Frings *et al.*, 2009; Makaske *et al.*, 2011).

Study limitations and future developments

An additional effect of floodplain aggradation not modelled here is that the vegetation, if not removed by desiccation, would in nature develop further towards a climax community, for instance as hardwood forest (Geerling *et al.*, 2006). This may also affect the bank stability as higher biodiversity and biomass may lead to better rooting and soil formation (Bätz *et al.*, 2015), while the denser forest causes much higher flow resistance to further reduce the probability of chute cutoffs. Such vegetation development depends partly on biogeographical conditions, which would make the models more context dependent and less generic. Nevertheless, our model partly represents a large number of bio-geomorphological processes

in rivers with combined effects of mud and vegetation. There is scope for improvements, such as positive effects of mud sedimentation on seedling survival because of the associated higher soil moisture and nutrient contents.

The quasi-periodic meander development and cutoff through a chute are mainly determined by the floodplain development on the entire inner-bend bar. While chute cutoffs limit the sinuosity, their failure or success depends on flood water levels, inner-bend bed elevation and hydraulic resistance (van Dijk *et al.*, 2014). This contrasts with scroll bar-dominated meandering rivers where the meander dynamics are mainly caused by the outer-bank erosion and also by along-channel sedimentation in the inner bend (Parker *et al.*, 2011; Schuurman, 2015), while neck cutoffs limit the sinuosity, which therefore usually becomes higher than in chute cutoff-dominated meandering rivers (Kleinhans and van den Berg, 2011). We therefore believe that the lack of proper cut-bank erosion processes in the model does not affect the main conclusions much. Likely the meander bend migration rate would differ as a function of rooting, but this is also sensitive to many model parameters including the parametrization of the transverse bed slope effect on sediment transport (Schuurman *et al.*, 2018). In case cohesive layers and rooting in the outer banks are important in reality, then inclusion of their effects in the numerical model would merely strengthen the observed trends, but results would be sensitive to a large number of empirical parameters. The inclusion of bank failure processes and effects of added bank strength from roots would perhaps allow modelling of meandering rivers with higher sinuosity and neck cutoffs. This would require further development of numerical techniques to represent layered and rooted banks that are much narrower than typical grid cells as subgrid features (e.g. Canestrelli *et al.*, 2016).

Implications for the Holocene floodplain and levee record

The implication of the results and discussion is that the entire range of river patterns from laterally stable, possibly anastomosing rivers to meandering and weakly braided rivers can occur in the given settings, and the resulting pattern depends strongly on upstream mud supply. Mud supply is an external forcing condition determined by the lithology, climate, vegetation and all other factors that determine the production and release of fine sediment from the hinterland. Vegetation cover, on the other hand, is a dependent variable that interacts with the bio-geomorphological pattern, rather than an independent variable that affects the river pattern (e.g., in ; Vandenberghe, 2008).

Reconstructions of Holocene river valleys and deltas emphasize the preserved lithology in channel belts and floodplains but make light of riparian vegetation (e.g. Erkens *et al.*, 2011). Riparian vegetation is only infrequently mentioned, likely because their remains are scarcely preserved in the oxidized environment of levees. Nevertheless, effects on river pattern of riparian vegetation on the levees could have been large. Pierik *et al.* (2017) suggest, on the basis of levee mapping in the entire Rhine delta, that levees were higher and narrower when vegetated, and became wider when riparian vegetation was cut down in the process of cultivation, notably in Roman times. This agrees with the present model results where vegetation captures floodplain sediment closer to the channel. However, the complexity of the modelled floodplain is partly due to the continuous connections with the channel, which would be more disconnected by high levees. The absence of a clear levee in the present modelling is likely due to the absence of multiple grain sizes between mud and coarse sand (e.g. (Cazanacli and Smith, 1998) but the tendency to form narrow levees in the presence of vegetation is demonstrated (Figure 9). Further modelling of levees with and without vegetation and in varying floodplain sizes along river valleys and deltas is required to test these hypotheses and improve reconstructions. Effects of roots in levees upon erosion and channel cutting are also understudied.

The spatial extent and detail of reconstructions in the Rhine hinterland and delta allowed an estimate that the floodplain sediment input increased in the past thousands of years due to removal of native vegetation and changing land use in the hinterland (e.g. Erkens *et al.*, 2011), which explains the accelerating levee growth (Pierik *et al.*, 2017). This shows that hillslope vegetation in the hinterland affects boundary conditions such as mud concentration, whereas riparian vegetation was part of the bio-geomorphological river system until humans removed it. While it demonstrates a clear effect of eco-engineering species on levee morphology, it remains unclear whether the rooting in the banks affected channel width and depth, meander migration rates and channel belt width. More in general, these results support the idea that fluvial style is mainly related to floodplain processes rather than channel processes, and that formation of levees is an important factor that in itself is partly determined by hinterland characteristics (see, for review, Kleinhans, 2010; Pierik *et al.*, 2017). These ideas may extend to deltas and estuaries that contain large volumes of mud in their substrates and floodplains. This mud may have filled accumulation space besides the channel, which could have had a similar effect to floodplain filling in rivers.

A model analogue for Palaeozoic rivers?

The gradual evolution of land plants in the early Paleozoic has been correlated with a global increase in mud deposition in fluvial facies and the increasing occurrence of facies associated with meandering and anastomosing river patterns (Davies *et al.*, 2011; Corenblit *et al.*, 2015; McMahon and Davies, 2018). However, the first land plants had no roots (Davies *et al.*, 2011). Since our model neglects effects of rooting on outer-bank erosion, this suggests that a comparison with Silurian and early Devonian rivers may shed new light on the recent debate about the specific eco-engineering effect of rootless land plants (Santos *et al.*, 2016; Davies *et al.*, 2017; McMahon and Davies, 2018).

We note, however, that the specific Allier river style without significant mud deposits near or in the channel and without recognizable lateral accretion surfaces, is irrelevant for the rock record, given the low preservation potential in this incisional setting. Therefore the active River Allier is not simplistically an appropriate analogue for Palaeozoic rivers interpreted from the rock record.

The debated problem is that the primitive plants at the time of the appearance of meandering fluvial styles had no significant roots that can have coped with desiccation and can have protected the banks against erosion (Santos *et al.*, 2016; Davies *et al.*, 2017; McMahon and Davies, 2018). However, our model scenarios demonstrate that plants can increase flow resistance and retain mud on the inner bend, regardless of their having roots, which enhanced the tendency to meander. The model scenarios thus support the hypothesis that the evolution of rootless land plants can have affected preserved fluvial facies. Specifically, this supports the hypothesis by Davies *et al.* (2011) and McMahon and Davies (2018) that the above-ground structure of newly evolved land

plants introduced a novel baffling effect, namely the trapping and deposition of muddy sediment. Even in the absence of rooting effects this mud is cohesive and elevates the floodplain to reduce strength of overbank flow, so that the rivers transform towards the laterally more stable patterns on the braiding–meandering–anastomosing continuum. Later development of roots in the Devonian introduced novel binding effects at the floodplain surface and in the erosive cut-banks that could have furthered the alluvial architectural changes.

The importance of rooting effects also varies with the size and pattern of present-day rivers. Results of Braudrick *et al.* (2009), van de Lageweg *et al.* (2014) and van Oorschot *et al.* (2016) show that rooted bank undercutting and retreat are of lesser importance for persistent meandering than the build-up of bars and prevention of chute cutoffs by vegetation on the bars. Here we argue that rooting will have been important in stabilizing banks in smaller rivers where root length approximates or even exceeds channel depth (Perona *et al.*, 2012), and in rivers where rooting leads to slump blocks that prevent bank toe erosion (Parker *et al.*, 2011). On the other hand, rooting cannot have been very important in large rivers with depths greatly exceeding root length, even if the pattern is similar. For example, the Ganges is chute cutoff dominated but its depth greatly exceeds root lengths. However, rivers of this size are rarely recognized in the rock record, with the exception of the McMurray formation meanders (Hubbard *et al.*, 2011). Rather, most fluvial systems recognized in Davies *et al.* (2011) to have been affected by vegetation are likely of the size of the River Allier and smaller, where the smaller systems are also more likely to occur further upstream in catchments. This illustrates the idea that small roots can have had significant binding effects on small rivers in the Palaeozoic.

Davies *et al.* (2011) and McMahon and Davies (2018) further hypothesize that rootless vegetation in the Palaeozoic has enhanced production of mud through chemical weathering in upland areas. Our modelling confirms that river pattern depends on mud supply, which requires that it is produced in quantity in the hinterland. These results and discussion point at the need to distinguish internal biomorphological processes in the river from external boundary conditions resulting from biomorphological processes in the hinterland in future interpretations of the rock record.

Conclusions

Two-dimensional numerical modelling of a laterally confined river with vegetation and/or mud was conducted, where mud was cohesive and where vegetation with all life stages caused hydraulic resistance. This led to the following insights.

For low mud concentration supplied at the upstream boundary, the river remained laterally mobile and cutoffs occurred frequently in the absence of vegetation. A high mud supply concentration stabilizes the floodplain and decreases the rate of channel migration and frequency of chute cutoffs because it fills floodplain lows and reduces overbank flow velocities. Higher mud concentrations led to meandering and, at extreme concentrations, high floodplain accretion with laterally stable channels that only occasionally avulsed, here interpreted as a tendency to form an anastomosing pattern.

Lateral confinement of the meander belt causes higher floodwater levels, which is further enhanced by the vegetation growth. This increases overbank flow, the rate of channel migration and frequency of chute cutoffs. Moreover, the high floodwater levels led to higher floodplain complexity and a shift toward a laterally more active and braided river planform pattern, contrary to the expected baffling effect of vegetation on river pattern. While vegetation locally reduces flow shear stress over the floodplain, the patchiness of vegetation causes a higher braiding index in winter during floods and a higher degree of dynamics expressed as channel migration and variations in sinuosity.

A novel quasi-periodic, hysteretic behaviour emerged in mud and vegetation cover. Chute cutoffs create windows of opportunity for vegetation settlement. Mud deposition lags behind because, in particular, the bushy vegetation efficiently reduces flow and captures mud.

Vegetation causes mud deposition closer to the main river channel to form levees. For higher mud concentrations, the increased floodplain dynamics due to vegetation are competed out by deposition. As a result, the floodplain fills up to reduce the flow strength, which, especially for higher cohesion of the floodplain sediment, hinders or even prevents chute cutoffs depending on mud concentration. At the highest mud concentration the floodplain fills up to such heights that the pioneer vegetation can no longer settle there or survive due to the lack of river water. These results imply that levee formation in Holocene river systems was enhanced and focused by riparian vegetation.

These results imply that primitive, rootless plants could have caused more frequent meandering patterns in Palaeozoic rivers. The mechanism may have been that hydraulic resistance by plants led to mud trapping, which, in turn, strengthened inner-bend floodplain through cohesion. This reduced the chute cutoff tendency and increased the tendency to meander, regardless of the absence of roots in erosive outer bends. This inner-bend effect of floodplain formation may also partly explain meandering in large rivers, where large bank height over root length ratios suggest insignificant outer-bank strengthening.

Acknowledgements—We gratefully acknowledge two anonymous reviews and steer by Special Issue Guest Editors. Discussions with Wout van Dijk, William McMahon, Harm Jan Pierik, Hans Middelkoop and Marcel van der Perk were much appreciated. MGK was supported by the European Research Council (ERC Consolidator grant 647570 to MGK). LB was supported a Vici grant by the Netherlands Organisation for Scientific Research (NWO, grant TTW 016.140.316 to MGK). MvO was supported by REFORM (FP7 Grant Agreement 282656 to Tom Buijse). The authors contributed in the following proportions to conception and design, data collection, modelling, analysis and conclusions, and manuscript preparation: MGK (40,0,0,50,50%), BdV (30,100,60,50,40%), LB (10,0,20,0,5%) and MvO (20,0,20,0,5%). The modelling was conducted by BdV as part of her MSc thesis (http://dspace.library.uu.nl/bitstream/handle/1874/362916/MScThesis_BentedeVries_CombinedEffectsOfMudAndRiparianVegetationOnRiverMorphology_def.pdf).

References

Baptist M, Babobic V, Rodriguez Uthurburu J, Keijzer M, Uittenbogaard R, Mynett A, Verwey A. 2006. On inducing equations for vegetation resistance. *Journal of Hydraulic Research* **45**: 1–16.

Bätz N, Verrecchia E, Lane S. 2015. The role of soil in vegetated gravelly river braid plains: More than just a passive response? *Earth Surface Processes and Landforms* **40**: 143–156.

Belliard J, Di Marco N, Carniello L, Toffolon M. 2016. Sediment and vegetation spatial dynamics facing sea-level rise in microtidal salt marshes: Insights from an ecogeomorphic model. *Advances in Water Resources* **93**: 249–264.

Bogaart P, van Balen R. 2000. Numerical modeling of the response of alluvial rivers to Quaternary climate change. *Global and Planetary Change* **27**: 147–163.

Bogoni M, Putti M, Lanzoni S. 2017. Modeling meander morphodynamics over self-formed heterogeneous floodplains. *Water Resources Research* **53**: 5137–5157.

Braat L, van Kessel T, Leuven J, Kleinhans M. 2017. Effects of mud supply on large-scale estuary morphology and development over centuries to millennia. *Earth Surface Dynamics* **5**: 617–652.

Braudrick C, Dietrich W, Leverich G, Sklar L. 2009. Experimental evidence for the conditions necessary to sustain meandering in coarse-bedded rivers. *Proceedings of the National Academy of Sciences* **106**: 936–941.

Caldwell R, Edmonds D. 2014. The effects of sediment properties on deltaic processes and morphologies: A numerical modeling study. *Journal of of Geophysical Research* **119**: 961–982.

Camporeale C, Perona P, Porporato A, Ridolfi L. 2007. Hierarchy of models for meandering rivers and related morphodynamic processes. *Reviews of Geophysics* **45**: 1001.

Canestrelli A, Spruyt A, Jagers B, Slingerland R, Borsboom M. 2016. A mass-conservative staggered immersed boundary model for solving the shallow water equations on complex geometries. *International Journal for Numerical Methods in Fluids* **81**: 151–177.

Cazanacli D, Smith N. 1998. A study of morphology and texture of natural levees: Cumberland Marshes, Saskatchewan, Canada. *Geomorphology* **25**: 43–55.

Corenblit D, Davies N, Steiger J, Gibling M, Bornette G. 2015. Considering river structure and stability in the light of evolution: feedbacks between riparian vegetation and hydrogeomorphology. *Earth Surface Processes and Landforms* **40**: 189–207.

Corenblit D, Steiger J, Charrier G, Darrozes J, Garófano-Gómez V, Garreau A, González E, Gurnell A, Hortobágyi B, Julien F, Lambs L, Larrue S, Otto T, Roussel E, Vautier F, Voldoire O. 2016a. Populus nigra L.establishment and fluvial landform construction: Biogeomorphic dynamics within a channelized river. *Earth Surface Processes and Landforms* **41**: 1276–1292.

Corenblit D, Vidal V, Cabanis M, Steiger J, Garófano-Gómez V, Garreau A, Hortobágyi B, Otto T, Roussel E, Voldoire O. 2016b. Seed retention by pioneer trees enhances plant diversity resilience on gravel bars: Observations from the river Allier, France. *Advances in Water Resources* **93**: 182–192.

Davies N, Gibling M, McMahon W, Slater B, Long D, Bashforth A, Berry C, Falcon-Lang H, Gupta S, Rygel M, Wellman C. 2017. Discussion on 'Tectonic and environmental controls on Palaeozoic fluvial environments: Reassessing the impacts of early land plants on sedimentation. *Journal of the Geological Society, London* **174**: 947–950.

Davies N, Gibling M, Rygel M. 2011. Alluvial facies evolution during the Palaeozoic greening of the continents: Case studies, conceptual models and modern analogues. *Sedimentology* **58**: 220–258.

Engelund F, Hansen E. 1967. *A Monograph on Sediment Transport in Alluvial Streams*. Teknisk Forlag: Copenhagen, Denmark.

Erkens G, Hoffmann T, Gerlach R, Klostermann J. 2011. Complex fluvial response to Lateglacial and Holocene allogenic forcing in the Lower Rhine Valley (Germany). *Quaternary Science Reviews* **30**: 611–627.

Ferguson R. 1987. Hydraulic and Sedimentary Controls of Channel Pattern. In *River Channels: Environment and Process*, Richards K (ed), Institute of British Geographers Special Publication 18. Blackwell: Oxford, UK; 129–158.

Filgueira-Rivera M, Smith N, Slingerland R. 2007. Controls on natural levee development in the Columbia River, British Columbia, Canada. *Sedimentology* **54**: 905–919.

Frings R, Berbee B, Erkens G, Kleinhans M, Gouw M. 2009. Human-induced changes in bed shear stress and bed grain size in the River Waal (The Netherlands) during the past 900 years. *Earth Surface Processes and Landforms* **34**: 503–514.

Geerling G, Ragas A, Leuven R, van den Berg J, Breedveld M, Liefhebber D, Smits A. 2006. Succession and rejuvenation in floodplains along the river Allier (France). *Hydrobiologia* **565**: 71–86.

Gran K, Paola C. 2001. Riparian vegetation controls on braided stream dynamics. *Water Resources Research* **37**: 3275–3283.

Guneralp I, Rhoads B. 2011. Influence of floodplain erosional heterogeneity on planform complexity of meandering rivers. *Geophysical Research Letters* **38**: L14401.

Gurnell A. 2014. Plants as river system engineers. *Earth Surface Processes and Landforms* **39**: 4–25.

Gurnell A, Bertoldi W, Corenblit D. 2012. Changing river channels: The roles of hydrological processes, plants and pioneer fluvial landforms in humid temperate, mixed load, gravel bed rivers. *Earth-Science Reviews* **111**: 129–141.

Hesselink A, Weerts H, Berendsen HJA. 2003. Alluvial architecture of the human-influenced river Rhine, The Netherlands. *Sedimentary Geology* **161**: 229–248.

Hubbard S, Smith D, Nielsen H, Leckie D, Fustic M, Spencer R, Bloom L. 2011. Seismic geomorphology and sedimentology of a tidally influenced river deposit, Lower Cretaceous Athabasca oil sands, Alberta, Canada. *AAPG Bulletin* **95**: 1123–1145.

Kleinhans MG. 2010. Sorting out river channel patterns. *Progress in Physical Geography* **34**: 287–326.

Kleinhans M G, de Haas T, Lavooi E, Makaske B. 2012. Network dynamics and origin of anastomosis in the upper Columbia River, Canada. *Earth Surface Processes and Landforms* **37**: 1337–1351.

Kleinhans MG, van den Berg JH. 2011. River channel and bar patterns explained and predicted by an empirical and a physics-based method. *Earth Surface Processes and Landforms* **36**: 721–738.

Lauer J, Parker G. 2008. Net local removal of floodplain sediment by river meander migration. *Geomorphology* **96**: 123–149.

Le Hir P, Cayocca F, Waeles B. 2011. Dynamics of sand and mud mixtures: A multiprocess-based modelling strategy. *Continental Shelf Research* **31**: 135–149.

Lesser GR, Roelvink JA, van Kester JATM, Stelling G. 2004. Development and validation of a three-dimensional morphological model. *Journal of Coastal Engineering* **51**: 883–915.

Lewin J, Ashworth P. 2014. The negative relief of large river floodplains. *Earth Science Reviews* **129**: 1–23.

Makaske B. 2001. Anastomosing rivers: A review of their classification, origin and sedimentary products. *Earth-Science Reviews* **53**: 149–196.

Makaske B, Maas G, van den Brink C, Wolfert H. 2011. The influence of floodplain vegetation succession on hydraulic roughness: Is ecosystem rehabilitation in Dutch embanked floodplains compatible with flood safety standards? *AMBIO* **40**: 370–376.

Makaske B, Smith D, Berendsen H, de Boer A, van Nielen-Kiezebrink M, Locking T. 2009. Hydraulic and sedimentary processes causing anastomosing morphology of the upper Columbia River, British Columbia, Canada. *Geomorphology* **111**: 194–205.

Matsubara Y, Howard A, Burr D, Williams RME, Dietrich W, Moore J. 2015. River meandering on Earth and Mars: A comparative study of Aeolis Dorsa meanders, Mars and possible terrestrial analogs of the Usuktuk River, AK, and the Quinn River, NV. *Geomorphology* **240**: 102–120.

McKenney R, Jacobson R, Wertheimer R. 1995. Woody vegetation and channel morphogenesis in low-gradient, gravel-bed streams in the Ozark Plateaus, Missouri and Arkansas. *Geomorphology* **13**: 175–198.

McMahon W, Davies N. 2018. Evolution of alluvial mudrock forced by early land plants. *Science* **359**: 1022–1024.

Mitchener H, Torfs H. 1996. Erosion of sand–mud mixtures. *Coastal Engineering* **29**: 1–25.

Nicholas A. 2013. Modelling the continuum of river channel patterns. *Earth Surface Processes and Landforms* **38**: 1187–1196.

Parker G, Shimizu Y, Wilkerson GV, Eke EC, Abad JD, Lauer JW, Paola C, Dietrich WE, Voller VR. 2011. A new framework for modeling the migration of meandering rivers. *Earth Surface Processes and Landforms* **36**: 70–86.

Perona P, Molnar P, Crouzy B, Perucca E, Jiang Z, McLelland S, Wüthrich D, Edmaier K, Francis R, Camporeale C, Gurnell A. 2012. Significance of the riparian vegetation dynamics on meandering river morphodynamics. *Water Resources Research* **43**: W03430.

Pierik H, Stouthamer E, Cohen K. 2017. Natural levee evolution in the Rhine–Meuse delta, the Netherlands, during the first millennium CE. *Geomorphology* **295**: 215–234.

Pollen-Bankhead N, Simon A. 2009. Enhanced application of root-reinforcement algorithms for bank-stability modeling. *Earth Surface Processes and Landforms* **34**: 471–480.

Roelvink J. 2006. Coastal morphodynamic evolution techniques. *Coastal Engineering* **53**: 277–287.

Santos M, Mountney N, Peakall J. 2016. Tectonic and environmental controls on Palaeozoic fluvial environments: Reassessing the

impacts of early land plants on sedimentation. *Journal of the Geological Society* **174**: 393–404.

Schuurman F. 2015. *Bar and channel evolution within meandering and braiding rivers using physics-based modeling. (Dissertation.) Utrecht Studies in Earth Sciences issue* **79**: 1–162.

Schuurman F, Marra W, Kleinhans MG. 2013. Physics-based modeling of large braided sand-bed rivers: Bar pattern formation, dynamics and sensitivity. *Journal of Geophysical Research* **118**: 2509–2527.

Schuurman F, Ta W, Post S, Sokolewicz M, Busnelli M, Kleinhans M. 2018. Response of braiding channel morphodynamics to peak discharge changes in the Upper Yellow River. *Earth Surface Processes and Landforms* **43**: 1648–1662.

Solari L, van Oorschot M, Belletti B, Hendriks D, Rinaldi M, Vargas-Luna A. 2016. Advances on modelling riparian vegetation–hydromorphology interactions. *River Research and Applications* **32**: 164–178.

Straatsma MW, Bloecker AM, Lenders HJR, Leuven RSEW, Kleinhans MG. 2017. Biodiversity recovery following delta-wide measures for flood risk reduction. *Science Advances* **3**: e1602762.

Struiksma N, Olesen K, Flokstra C, De Vriend H. 1985. Bed deformation in curved alluvial channels. *Journal of Hydraulic Research* **23**: 57–79.

Tal M, Paola C. 2010. Effects of vegetation on channel morphodynamics: Results and insights from laboratory experiments. *Earth Surface Processes and Landforms* **35**: 1014–1028.

Temmerman S, Bouma T, van de Koppel J, van der Wal D, de Vries M, Herman P. 2007. Vegetation causes channel erosion in a tidal landscape. *Geology* **35**: 631–634.

van Dijk W, Schuurman F, Van de Lageweg W, Kleinhans M. 2014. Bifurcation instability and chute cutoff development in meandering gravel-bed rivers. *Geomorphology* **213**: 277–291.

van Dijk W, Teske R, van de Lageweg W, Kleinhans MG. 2013a. Effects of vegetation distribution on experimental river channel dynamics. *Water Resources Research* **49**: 7558–7574.

van Dijk WM, Van de Lageweg WI, Kleinhans MG. 2012. Experimental meandering river with chute cutoffs. *Journal of Geophysical Research* **117**: F03023.

van Dijk WM, Van de Lageweg WI, Kleinhans MG. 2013b. Formation of a cohesive floodplain in a dynamic experimental meandering river. *Earth Surface Processes and Landforms* **38**: 1550–1565.

van Kessel T, Vanlede J, de Kok J. 2011. Development of a mud transport model for the Scheldt estuary. *Continental Shelf Research* **31**: 165–181.

van Ledden M, van Kesteren W, Winterwerp J. 2004. A conceptual framework for the erosion behaviour of sand–mud mixtures. *Continental Shelf Research* **24**: 1–11.

van Oorschot M, Kleinhans MG, Geerling GW, Egger G, Leuven RSEW, Middelkoop H. 2017. Modeling invasive alien plant species in river systems: Interaction with native ecosystem engineers and effects on hydro-morphodynamic processes. *Water Resources Research* **53**: 6945–6969.

van Oorschot M, Kleinhans M, Geerling G, Middelkoop H. 2016. Distinct patterns of interaction between vegetation and morphodynamics. *Earth Surface Processes and Landforms* **41**: 791–808.

van de Lageweg W, van Dijk W, Baar A, Rutten J, Kleinhans M. 2014. Bank pull or bar push: What drives scroll-bar formation in meandering rivers? *Geology* **42**: 319–322.

van der Wegen M, Dastgheib A, Roelvink J. 2010. Morphodynamic modeling of tidal channel evolution in comparison to empirical pa relationship. *Coastal Engineering* **57**: 827–837.

Vandenberghe J. 2008. The fluvial cycle at cold–warm–cold transitions in lowland regions: A refinement of theory. *Geomorphology* **98**: 275–284.

Winterwerp J, van Kesteren W. 2004. *Introduction to the Physics of Cohesive Sediment in the Marine Environment*, No.56 in Developments in Sedimentology. Elsevier: Amsterdam.

Supporting Information

Supporting information may be found in the online version of this article.